MULTI-OBJECTIVE OPTIMIZATION OF OPERATING PARAMETERS OF A PEM FUEL CELL UNDER FLOODING CONDITIONS USING THE NON-DOMINATED SORTING GENETIC ALGORITHM (NSGA-II)

Hamid ABDI[1,3], Noureddine AIT MESSAOUDENE[2,3], Lioua KOLSi[2,4*] and Messaoud BELAZZOUG[5]

[1]Département de Mécanique University of Blida 1, P.O. Box 270. Blida, Algeria
[2] Department of Mechanical Engineering, University of Hail, Saudi Arabia.
[3]Laboratoire des Applications Energétiques de l'Hydrogène (LApEH), University of Blida 1, Algeria
[4]Unité de Métrologie et des Systèmes Énergétiques, École Nationale d'Ingénieurs, Monastir, University of Monastir, Tunisia
[5]Laboratory of Electric Systems and Telecommand (LABSET), University of Blida 1, Algeria
*Corresponding author, e-mail: lioua_enim@yahoo.fr

In the present study, the performance of a PEMFC is studied under cathode flooding conditions. A two-dimensional model of water and heat management based on the laws of conservation and electrochemical equations is used. The performance of the PEM cell is evaluated on the basis of the computed average current density and its distribution along the channels. Operating parameters are optimized with the objective of maximizing average current density while minimizing its variations. The problem is formulated into a multi-objective form that is solved by the Non-dominated Sorting Genetic Algorithm (NSGA-II) to find the optimal Pareto front. The results of the base case are compared to those of the optimized cell. A 38.94% increase in average current density and a 38.8% decrease in standard deviation are obtained.

Key words: *PEMFC, Cathode flooding, NSGA-II, Current-voltage characteristic*

1. Introduction

Proton exchange membrane fuel cells (PEMFC) exhibit many desirable features such as low operating temperature, short start time and relatively high levels of efficiency and durability within the fuel cell technology. Therefore, PEM fuel cells focus an important part of research and development. For instance, they are almost universally chosen to equip fuel cell vehicles of the future [1]. For example, Malekbala *et al.* [2], have studied the effects of several operating parameters of the fuel cell system. The obtained results show that the proposed model can predict the dynamic behavior of the fuel cell system.

Understandably, a great deal of research effort has been focused on PEMFC basic aspects and the advancement of its technology. However, improving in fuel cell durability is still confronted with significant challenges [3]. The non-uniform current distribution in PEMFC results in accelerated ageing, local overheating, power output and performance degradation [4-6]. In addition, operating under flooding conditions causes a non-uniform distribution of the current in a PEMFC. Flooding is a

dominant factor that limits a PEMFC performance, especially for high current densities. In this case, the excessive quantity of water produced condenses and fills the electrode pores; this is called water flooding. The transport of reactants to the active catalyst surface is therefore restrained. Understanding the relation between this phenomenon of excess liquid water and spatial current profile is crucial for the design and operation of PEMFCs [7].

Improving the performance PEMFC's requires investigating and understanding of the interacting parameters and their effects on performance. These include geometrical as well as operating parameters. The geometric parameters of the cell are very important but are not considered as variables during the use of a given cell. On the other hand, an adequate choice of operating parameters can result in a high power density cell and an extension of its life. Fuel cell parameters optimization has been the subject of several research studies. The core of fuel cell modeling work presented by Sedighizadeh *et al.* [8] is to identify model parameters using the particle swarm optimization (PSO) method in association with fitting the model to experimental data. A model based on electrochemical reactions occurring in a PEMFC is presented by Askarzadeh and Rezazadeh [9]. In order to improve the accuracy of this model so that it can better reflect the actual PEMFC performance, its parameters are optimized by means of a modified particle swarm optimization (MPSO). A genetic algorithm-polynomial neural network (GA-PNN) is used for modeling PEMFC performance. It is based on numerical results which are correlated with experimental data and have been proposed by Mehrabi *et al.* [10]. Tafaoli-Masoule *et al.* [11] have presented optimum design parameters and operating conditions for maximum power of a direct methanol fuel cell using analytical model and genetic algorithm. In addition, Yang *et al.* [12] present the use of genetic algorithm (GA) to optimize the bipolar plate channel geometry of a PEMFC. Sun *et al.* [13] have proposed a hybrid adaptive differential evolution algorithm (HADE) for identifying nonlinear parameters of PEMFC. Through experimental comparison with other identified methods, the PEMFC model based on HADE algorithm shows better performance. Al-Othman *et al.* [14] have presented parametric identification of PEMFC using quantum-based optimization method (QBOM). The proposed method is applied to a 1.2kW Ballard Nexa fuel cell to identify the exact parameters and has successfully been tested experimentally. Results based on parameter identification, simulation and experimental measurements are compared for validation purposes. Haghighi *et al.* [15] have analyzed the exergy of a high temperature PEMFC. In this work a genetic algorithm code is developed using MATLAB software to compute and optimize work, exergy, exergy efficiency and thermodynamic irreversibility. Chen *et al.* [16] have introduced a novel multi-objective evolutionary algorithm based on decomposition (MOEA/D) to optimize the operating parameters of the PEMFC system for the purpose of maximizing system efficiency and power. Rao *et al.* [17] have presented an optimization of operating parameters to maximize the current density without flooding at the cathode membrane interface of a PEM fuel cell using Taguchi method and genetic algorithm. Boudouh *et al.* [18] have presented experimental results of a study of the phase change cooling using forced convection flow in mini-channels. The prototype is designed to simulate PEMFC cooling.

Optimization of the operating parameters of the PEMFC under partial flooding conditions of the cathode has not been clearly addressed in the literature. Among the works that focus on the study of the effect of water flooding on non-uniform distribution of current in PEM cells, a noteworthy contribution has recently been performed by Karimi *et al.* [19]. They present a study designed to determine PEM fuel cell performance under flooding conditions. A two-dimensional approach based

on the laws of conservation and electrochemical equations is proposed; the mechanisms of water generation and transfer and how they affect the performance of the cell are illustrated. In the same context, Jamekhorshid *et al.* [20] have proposed a two-dimensional model of partial flooding of the gas diffusion layer for studying local current density profiles along the flow pathway over a wide range of operating conditions.

In the present work, a two-dimensional model of heat and water management based on the laws of conservation and electrochemical equations is used for studying the performance of a PEMFC. Special attention is given to flooding conditions. In order to improve previous optimization models, the Non-dominated Sorting Genetic Algorithm (NSGA-II) is also used for optimizing operating parameters with regard to cell performance and durability.

2. Mathematical model

A PEMFC is depicted in figure 1. It actually is an assembly of membrane and electrodes (MEA). An electrolyte membrane is placed in the middle of two pairs of catalyst and micro-porous gas diffusion layers (GDL).

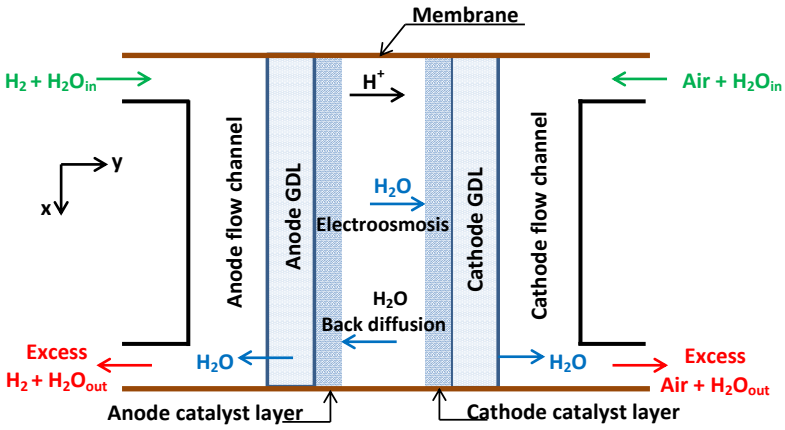

Figure 1. Schematic illustration of the PEMFC.

The mathematical model and assumptions developed in different studies [19-21] are used in the present; it is a quasi-stationary two-dimensional model with partial flooding of the GDL diffusion layer. It reflects the heat and mass transfer occurring in a PEMFC.

2.1. Governing equations

Under quasi-stationary conditions, local current densities are set by the reactant molar flow rates when transported through flow channels to the chemical reaction sites. The molar flow rates for various species and water vapor, at a local position (x) along the flow channel, are given by:

$$\frac{dN_i(x)}{dx} = \xi_i \frac{w\, I(x)}{4F} \tag{1}$$

Anode channel: $\xi_{H_2} = -2,\ \xi_{w,a} = -4\alpha$

Cathode channel: $\xi_{O_2} = -1,\ \xi_{w,c} = 2 + 4\alpha,\ \xi_{N_2} = 0$

The parameter α represents the net water molecule per proton flux ratio, which is taken as:

$$\alpha = n_d - \frac{F}{I(x)} D_w \frac{dC_w}{dy} - C_w \frac{k_p}{\mu} \frac{F}{I(x)} \frac{dP_w}{dy} \tag{2}$$

In order to minimize the complexity of this model, it is assumed that both water concentration and pressure gradients, across the membrane, are approximated by linear variation constants. The expression of α becomes:

$$\alpha = n_d - \frac{F}{I(x)} D_w \frac{C_{w,c} - C_{w,a}}{t_m} - \frac{(C_{w,c} + C_{w,a})}{2} \frac{k_p}{\mu} \frac{F}{I(x)} \frac{(P_{w,c} - P_{w,a})}{t_m} \tag{3}$$

Where n_d, D_w, k_p, μ and t_m are the electro-osmotic coefficient (number of water molecules carried by a proton), water diffusion coefficient, permeability of water in the membrane, water viscosity and membrane thickness, respectively,

Water vapor flow rate variation along the flow channels depends on both liquid water flow rate variation and water vapor flux into and out of the membrane.

Anode:

$$\frac{dN^l_{w,a}(x)}{dx} = \left(\frac{k_c\ h\ w}{R(T_a(x) + 273)} \right) \left(\frac{N^v_{w,a}(x)}{N^v_{w,a}(x) + N_{H_2}(x)} P_a(x) - P^{sat}_{w,a}(x) \right) \tag{4}$$

$$\frac{dN^v_{w,a}(x)}{dx} = -\left(\frac{dN^l_{w,a}(x)}{dx} \right) - \frac{w\ \alpha\ I(x)}{F} \tag{5}$$

Cathode:

$$\frac{dN^l_{w,c}(x)}{dx} = \left(\frac{k_c\ h\ w}{R(T_c(x) + 273)} \right) \left(\frac{N^v_{w,c}(x)}{N^v_{w,c}(x) + N_{O_2}(x) + N_{N_2}(x)} P_c(x) - P^{sat}_{w,c}(x) \right) \tag{6}$$

$$\frac{dN^v_{w,c}(x)}{dx} = -\left(\frac{dN^l_{w,c}(x)}{dx} \right) + \frac{w\ I(x)\ (1 + 2\alpha)}{2F} \tag{7}$$

where k_c is the rate constant for evaporation and condensation of water; h and w are respectively the height and width of the channel.

The energy balance equation of the gas mixture at the anode and cathode is given by:

$$\sum_i (N_i(x) C_{p,i} \frac{dT_k(x)}{dx} = (H^v_{w,k} - H^l_{w,k}) \frac{dN^l_{w,k}(x)}{dx} + U\ a\ (T_s - T_k(x)) \tag{8}$$

where U is the overall heat transfer coefficient, a is the heat exchange area per unit length of the channel ($a = 2\ (h+w)$).

The cell potential is calculated by subtracting the activation polarization and the Ohmic polarization from the open circuit voltage as follows:

$$E_{cell} = E_{oc} - \eta_{act}(x) - \eta_{ohm}(x) \tag{9}$$

E_{oc} is given by:

$$E_{oc} = 1.229 - 0.85 \times 10^{-3} (T_s - 298.15) + 4.31 \times 10^{-5} T_s \left[\ln P_{H_2}(x) + \frac{1}{2} \ln P_{O_2}(x) \right] \tag{10}$$

$\eta_{act}(x)$ is expressed by the following equation:

$$\eta_{act}(x) = \frac{R\ (273 + T_s)}{0.5\ F} \ln \left(\frac{I(x)}{(I^o P^{cat}_{O_2}(x)} \right) \tag{11}$$

I^0 is the exchange current density at 1 atmosphere of oxygen, $P^{cat}_{O_2}(x)$ is the oxygen partial pressure at the catalyst interface of the GDL. Assuming an ideal gas mixture, $P^{cat}_{O_2}(x)$ is given by:

$$P^{cat}_{O_2}(x) = C^{cat}_{O_2}(x)\ R\ (T_c(x) + 273) \tag{12}$$

The relation between oxygen concentration at the catalyst surface, $C_{O_2}^{cat}(x)$, and oxygen concentration in the flow channels is described by:

$$C_{O_2}^{cat}(x) = C_{O_2}^{bulk}(x) - \frac{I(x)}{4F}\left(\frac{1}{h_{O_2}} + \frac{t_{GDL}}{D_{O_2-g}^{eff}}\right) \tag{13}$$

The effective diffusion coefficient, $D_{O_2-g}^{eff}$, is given by:

$$D_{O_2-g}^{eff} = D_{O_2-g}\left[(1-s)\,\phi\right]^{3/2} \tag{14}$$

where *s* is liquid water saturation parameter. It is defined as the fraction of the overall GDL void space occupied by liquid water. It is given as follows:

$$s = \frac{(P_{w,c}(x) - P_{w,c}^{sat}(x))\;\; M_w}{R\,(T_c(x) + 273)\,\rho_w} \tag{15}$$

The ideal gas law is used to calculate the oxygen concentration in the flow channel:

$$C_{O_2}^{bulk}(x) = \frac{P_{O_2}(x)}{R\;\;(T_c(x) + 273)} \tag{16}$$

The mass transfer coefficient of oxygen h_{O_2} can be approximated by assuming a mass transfer for fully developed laminar flow through a three-sided adiabatic square sectioned duct with constant mass flux applied at one face:

$$Sh = \frac{h_{O_2}\;D_k}{D_{O_2-g}} = 2.7 \tag{17}$$

where the oxygen diffusion coefficient is given by:

$$D_{O_2-g} = \frac{1 - Y_{O_2}}{(Y_{N_2} / D_{O_2-N_2}) + (Y_{w,v,c} / D_{O_2-w,v})} \tag{18}$$

Y_{O_2} , Y_{N_2} *and* $Y_{w,v,c}$ respectively are the mole fractions of oxygen, nitrogen and water vapor. Oxygen diffusion coefficients in water vapor and nitrogen ($D_{O_2-w,v}$, $D_{O_2-N_2}$) are given by:

$$D_{O_2-w,v} = D_{O_2-w,v}^{std}\left(\frac{T_c(x) + 273}{273}\right)^{2/3}\left(\frac{1}{P_c(x)}\right) \tag{19}$$

$$D_{O_2-N_2} = D_{O_2-N_2}^{std}\left(\frac{T_c(x) + 273}{273}\right)^{2/3}\left(\frac{1}{P_c(x)}\right) \tag{20}$$

Ohmic polarization is given by: $$\eta_{ohm}(x) = \frac{I(x)t_m}{\sigma_m(x)} \tag{21}$$

The average current density is given by: $$I_{avg} = \frac{1}{L}\int_0^L I(x)dx \tag{22}$$

The complementary empirical equations used in this model are described in details in the work of Nguyen and White [21].

2.2. Computational procedure

In order to solve the governing equations of the heat and mass transfer in the PEMFC, two options are available; namely, maintaining a constant average current density or a constant voltage. In this work, the second option is adopted.

The set of governing equations is solved numerically as follows:

- The cell voltage is predefined.

- The flow channels for the anode and cathode are meshed into a number of equal elements.
- The average current density I_{avg} is specified. Based on I_{avg}, molar flow rates of hydrogen, oxygen and water vapor are calculated at the entrance of the flow channel.
- Computations start from the first element for which the local current density *I(x)* is also assumed.
- The governing equations of mass and heat transfers in the anode and cathode are solved for the first element.
- Then the voltage is computed. If this value of voltage differs from the present value, the local current density must be corrected. An iteration loop based on the Newton-Raphson method is used to find the correct local current density. Otherwise, computations are performed for the next segment.
- This procedure is repeated until computations for all segments of the channel are completed.
- Then, the mean current density I_{avg} is computed and compared with the specified value. If the difference exceeds a specified convergence criterion, I_{avg} is corrected; otherwise, computations are stopped.

3. Optimization formulation

Multi-objective optimization methods have been used in different problems, with relatively low focus on PEMFC [22, 23]. Several research works have been devoted to study the effects of main operating conditions on PEMFC performance [19, 20]. From a useful point of view, the performance of a PEM cell must be evaluated on the basis of the average current density as well as its variation along the channels. In general, the desired target is a high average current density with lowest variations, measured by standard deviation. The first requirement guarantees a high power density, while the latter is necessary for the durability of the system. Indeed, decreasing the level of current variability has a positive impact on cell durability as it prevents local overheating, which causes a degradation of both durability and power output. The two desired objectives are grouped into one objective function for optimizing the operating parameters of the PEMFC. This analysis results in a unique solution [24].

However, in our work, the problem of maximizing the average current density and minimizing the standard deviation is formulated in multi-objective form that is solved by the NSGA-II method. This algorithm gives a set of solutions, each representing a compromise between the different objectives to be optimized [25]. It is based on the classification of individuals into several levels and uses a faster sorting procedure based on non-dominance or optimal Pareto. This latter is an elitist approach that preserves the diversity of populations, securing best solutions found in previous generations on one hand and using a comparative operator based on calculating the Crowding distance on the other hand. Detailed description of NSGA-II is given elsewhere [25].

The NSGA-II algorithm is used for optimizing the PEMFC operating parameters. The objective is to maximize power density and minimize current density variability along the flow direction in the cell. The objective functions considered are the following:

$$Fobj_1 = \max.(I_{avg}) \text{ and } Fobj_2 = \min.(Sd) \tag{23}$$

I_{avg} is the average current density along the flow channel and *Sd* its standard deviation given by:

$$Sd = \sqrt{\frac{\sum_{j=1}^{n} (I(x_j) - I_{avg})^2}{n}} \tag{24}$$

Where n represents the number of node along the canal.

To solve this problem, the NSGA-II algorithm is used. The selected values of various parameters of NSGA-II used in this work are: population size: 400, number of generation: 1000, crossover probability: 80% and mutation probability: 10%

The values of decision variables lower and upper limits selected for the present computations are shown in Table 3.

4. Results and discussion

Before going further in our analysis, it is important to test the validity of our simulation results. Figure 2 shows a comparison of simulation results for the current density profile from the present model with simulation results from Jamekhorshid *et al.* [20] obtained for similar operating conditions, i.e.: hydrogen and air inlet temperature: 80°C; cell temperature: 80°C; anode stoichiometry: S_a =1.2; cathode stoichiometry: S_c =1.75; anode inlet relative humidity: 100%; cathode inlet relative humidity: 85%. It can be seen that the prediction of the present study is in reasonable agreement with results from Jamekhorshid *et al.* [20]. The slight difference can be attributed to the fact that the model presented by Jamekhorshid *et al.* [20] assumes isothermal operating conditions.

Table 3. Upper and lower limits values of the parameters to be optimized.

Parameter	Lower value	Upper value
Cell temperature, T_s, [°C]	60	80
Inlet temperature of anode gas, T_a^{in}, [°C]	60	80
Inlet temperature of cathode gas, T_c^{in}, [°C]	60	80
Inlet pressure of anode, P_a^{in}, [atm]	1.5	3
Inlet pressure of cathode, P_c^{in}, [atm]	1.5	3
Inlet anode humidity, RH_a^{in}, [%]	50	100
Inlet cathode humidity, RH_c^{in}, [%]	50	100
Anode stoichiometry, S_a, [–]	1.2	1.8
Cathode stoichiometry, S_c, [–]	1.8	2.5

4.1. Base case

The base case corresponds to a PEMFC operating with pure hydrogen and air at 1.5 atm, a temperature of 70 °C and a voltage of 0.6 V. At both inlets, cathode and anode, gaseous mixtures are considered to be saturated with water vapor. The entrance humidification temperature is considered equal to the PEMFC temperature. The input parameters and properties used in computations for the base case are taken from Karimi et al [19] and Nguyen and White [21].

Figure 3 shows the contribution of each water transport mechanism, including net water flux per proton (α), electro-osmotic drag coefficient (n_d), diffusion flux due to concentration gradient of water vapor and the convective flux that is due to the pressure gradient of water vapor. The contribution of the convective flux is very small (close to zero as shown in fig. 3). Near the fuel cell inlet, the electro-osmotic drag coefficient (n_d) and net water flux per proton (α) are very high. This is due to the fact that the membrane is well hydrated. The transport of water by diffusion is from cathode side to anode side. It should be noted that diffusion water transport through the membrane depends solely on water concentration gradient across the membrane. The variations of the other parameters of the PEM fuel cell (base case) are presented in Fig. 5.

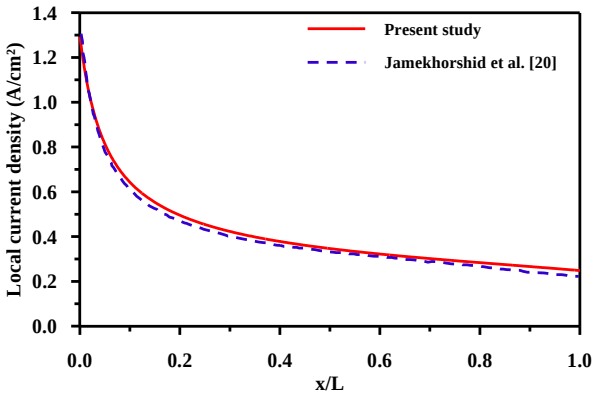

Figure 2. Comparison between the our simulation results and simulation results from Jamekhorshid *et al*. [20] (RH_c^{in} = 85%, RH_a^{in} = 100%, S_c = 1.75, S_a = 1.2, P_c^{out} = 1 atm, T = 80°C).

4.2. Optimization results

The result of the optimal Pareto front is shown in Fig. 4. It clearly shows that the basic case study represented by point (D) does not belong to non-dominated solutions. The two objective functions are antagonistic; improvement in average current density causes an increase in standard deviation. A good distribution of solutions on the Pareto front can also be observed. Table 4 illustrates the solution (B), the two extreme solutions (A) and (C), and the base case. Point (A) is an optimum result corresponding to the case where current density standard deviation is assumed as the only objective function. Similarly, point (C) is an optimum result where average current density is considered as the single objective function.

The operating parameters as well as the results obtained for the basic case and the optimized cell (point B) are presented in Table 5. It is found that the average current density of the optimized cell increases by 38.94% and the standard deviation decreases by 38.8%.

Figure 5 (a-g) shows the variation of various parameters of the PEM cell along the flow channel for both the base case and the optimized cell. The improvement in current density is clearly demonstrated in Fig. 5(a). In the basic case, the current density is higher at the inlet; this is due to the fact that the gases are more humidified compared to the case of the optimized cell.

The same can be said for the ionic conductivity profile as shown in Fig. 5(b). Water transfer from anode to cathode causes a decrease in water activity at the anode for the base case (Fig. 5(c)), a decrease in net transport coefficient of water molecules per proton (Fig. 5(d)) and a decrease in membrane ionic conductivity. Moreover, accumulation of liquid water at the cathode (Fig. 5(e)), caused by the electrochemical reaction and water migration from anode to cathode, leads to partial flooding of the cathode (Fig. 5(f)). Under these flood conditions, liquid water filling the pores of GDL's and limiting the transport of oxygen to the active surface of the catalyst causes a decrease in current density. An increase in gas mixture temperature is also noted at the cathode (Fig. 5(g)). It is due to the latent heat of condensation of water. On the other hand, the temperature of the gaseous mixture at the anode is kept constant because the gases enter at the temperature of the cell and no phase change has occurred yet.

Table 4. Comparison of three selected non-dominated solutions on the optimal Pareto curve and the base case.

	A	B	C	D
I_{avg}, [Acm^{-2}]	0.7476	1.0746	1.2982	0.7734
Sd, [Acm^{-2}]	0.0197	0.1571	0.4474	0.2567

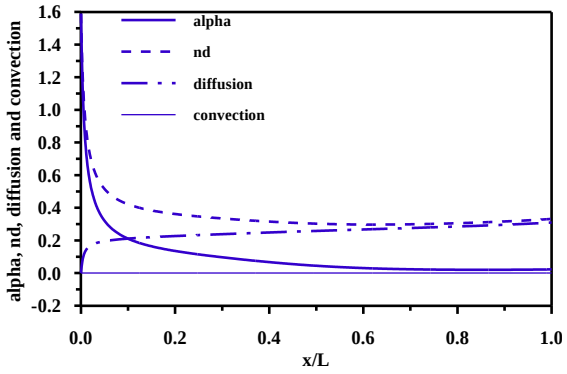

Figure 3. Variation along the channel of water transport mechanisms.

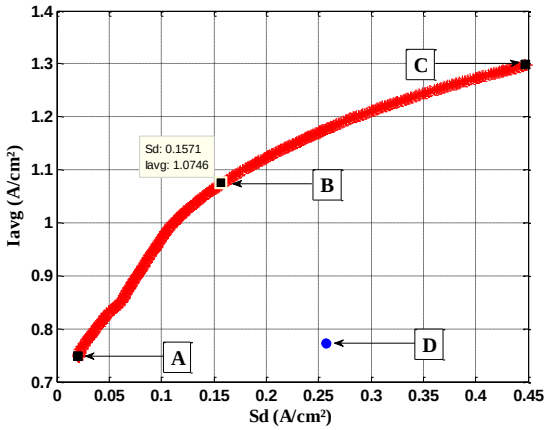

Figure 4. The distribution of Pareto-optimal solution (Pareto front) using NSGA-II where average current density and standard deviation of the current density as two objective functions.

Table 5. Decision variables and objective function values of the PEMFC before and after optimization.

	Base cell	Optimized cell
Decision variables		
Cell temperature, T_s, [°C]	70	80
Inlet temperature of anode gas, T_a^{in}, [°C]	70	80
Inlet temperature of cathode gas, T_c^{in}, [°C]	70	70.93
Inlet pressure of anode, P_a^{in}, [atm]	1.5	1.5
Inlet pressure of cathode, P_c^{in}, [atm]	1.5	3
Inlet anode humidity, RH_a^{in}, [%]	100	61.11
Inlet cathode humidity, RH_c^{in}, [%]	100	98.43
Anode stoichiometry, S_a, [–]	1.2	1.8
Cathode stoichiometry, S_c, [–]	1.8	2.5
Objective function		
I_{avg}, [Acm^{-2}]	0.7734	1.0746
Std, [Acm^{-2}]	0.2567	0.1571
Molar flow rate		
Inlet molar flow rate of hydrogen, [mols^{-1}]	9.62x10^{-6}	2.0x10^{-5}
Inlet molar flow rate of water vapor at the anode, [mols^{-1}]	2.46x10^{-6}	4.67x10^{-6}
Inlet molar flow rate of oxygen, [mols^{-1}]	7.22x10^{-6}	1.39x10^{-5}
Inlet molar flow rate of water vapor at the cathode, [mols^{-1}]	8.78x10^{-6}	7.72 x10^{-6}

Despite an increase of molar flow rates of hydrogen and water vapor at the inlet of the anode channel for the optimized cell, Figs. 5(b), (c) and (d) show that activity of water at the anode, membrane conductivity and net transport coefficient of water molecules per proton are higher for the basic case. This can be attributed to the fact that the gaseous mixture is completely saturated near the

inlet of the anode. In the remaining part of the channel, higher relative humidity at the anode of the optimized cell results in an increase in net water transfer coefficient per proton and higher membrane conductivity. Consequently, this leads to higher current density compared to the base case (Fig. 5(a)). Moreover, a lower gas mixture temperature at the cathode for $x/L < 0.32$ with respect to cell temperature (Fig. 5(g)) can reduce the generation of liquid water at the cathode and consequently the degree of saturation in liquid water as shown in Figs. 5(e) and (f) respectively. A zero liquid water saturation for $x/L < 0.12$ for the optimized cell can be explained by the fact that water vapor pressure at the cathode is lower than the saturation pressure.

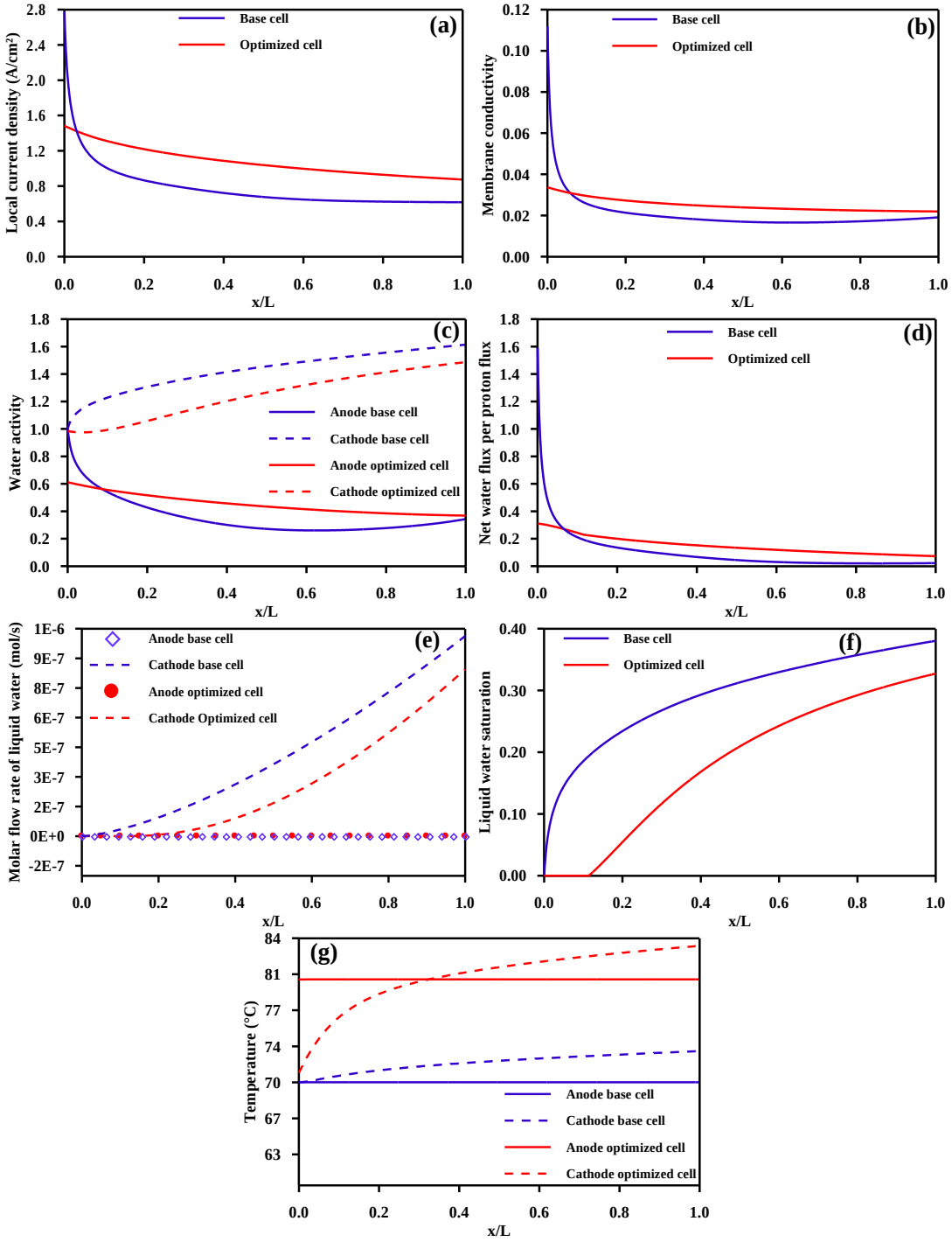

Figure 5. Variation along the channel of : (a) current density; (b) membrane conductivity ; (c) water activity ; (d) net water per proton flux; (e) molar flow rate of liquid water; (f) liquid water saturation; (g) gaseous mixture temperature for base and optimized cells.

5. Conclusion

PEMFC performance under flooded cathode conditions is studied. A two-dimensional mathematical model simulating the management of water and heat based on the laws of conservation and electrochemical equations is used. The operating parameters of a PEM unit cell have been optimized using the NSGA-II algorithm. The double objective is to obtain the highest power density possible while minimizing current density variations along the channel. The end result of the optimization process is no longer given by a single solution but rather by a set of solutions.

A comparison of the results obtained through the optimization algorithm NSGA-II with the base case is performed. One of the non-dominated solutions on the optimal Pareto curve is selected for this purpose. This solution satisfies the two objectives namely, a higher average current density and a lower standard deviation. It is found that average current density of the optimized cell increases by 38.94% and the standard deviation decreases by 38.8%. Furthermore it is noted that the risk of cathode flooding is reduced.

Nomenclature

a – heat transfer area per unit length, [cm]
a_k – activity of water in stream k, [–]
c – concentration, [molcm^{-3}]
$C_{P,i}$ – heat capacity of gas i, [Jmol^{-1}°C^{-1}]
D – diffusion coefficient, [cm²s^{-1}]
D_k – hydraulic diameter, [cm]
E – cell voltage, [V]
F – Faraday's constant, [Cmol^{-1}]
h – channel height, [cm]
h – convective mass transfer coefficient, [cms^{-1}]
H – enthalpy, [Jmol^{-1}]
I – local current density, [Acm^{-2}]
I_{avg} – cell average current density, [Acm^{-2}]
I^0 – exchange current density for the oxygen reaction, [Acm^{-2}]
k_c – evaporation and condensation rate constant, [s^{-1}]
k_p – hydraulic water permeability, [cm^2]
L – channel length, [cm]
$M_{m,dry}$ – equivalent weight of a dry membrane, [gmol^{-1}]
M_w – molecular weight, [gmol^{-1}]
N – molar flux, [mols^{-1}]
N_i – molar flow rate of species i, [mols^{-1}]
n_d – electro-osmotic drag coefficient, [–]
P – pressure, [atm]
R – gas constant, [Jmol^{-1}K^{-1}] or, [atmcm^{3}K^{-1}mol^{-1}]
RH – relative humidity, [%]
s – liquid saturation, [–]
S – stoichiometry coefficient, [–]
Sh – Sherwood number, [–]
t – thickness, [cm]
T – cell temperature, [°C]
T_s – temperature of the solid phase, [°C]
U – overall heat-transfer coefficient, [Js^{-1}cm^{-2}°C^{-1}]
w – channel width, [cm]
x – direction along the channel length, [cm]
y – direction normal to the channel length, [cm]
Y – molar fraction, [–]

Greek Symbols

α – net water flux per proton flux, [–]
η – overpotential, [V]
μ – viscosity, [kgcm^{-1}s^{-1}]
ξ – stoichiometric coefficient, [–]
ρ – density, [gcm^{-3}]
$\rho_{m,dry}$ – dry membrane density, [gcm^{-3}]
σ – membrane conductivity, [Ω^{-1}cm^{-1}]
φ – GDL porosity, [–]

Subscripts/Superscripts

a – anode
act – activation
avg – average
c – cathode
cat – catalyst
eff – effective
g – gas phase
GDL – gas distribution layer
H_2 – hydrogen
i – component
in – inlet
k – anode/cathode
m – membrane
N_2 – nitrogen
O_2 – oxygen
oc – open circuit
ohm – ohmic
sat – saturation
std – standard
v – vapor
w – water

References

[1] Ait Messaoudene N., *et al.*, Estimation of Indirect CO_2 Emissions of a Hydrogen Powered Medium Size Vehicle for the NEDC cycle, *International Journal of Energy Research, 34* (2010), pp. 745-756

[2] Malekbala, M.R., Modeling and Control OF A Proton Exchange Membrane Fuel Cell with the Air Compressor According to Requested Electrical Current, *Thermal Science, 19* (2015), 6, pp. 2065-2078

[3] Hwang, J.J., *et al.*, Development of a Lightweight Fuel Cell Vehicle, *Journal of Power Sources*, *141* (2005), 1, pp. 108-115
[4] Cleghorn, S.J.C., *et al.*, A Printed Circuit Board Approach to Measuring Current Distribution in a Fuel Cell, *Journal of Applied Electrochemistry*, *28* (1998), 7, pp. 663–672
[5] Weng, F.B., *et al.*, Numerical Prediction of Concentration and Current Distributions in PEMFC, *Journal of Power Sources*, *145* (2005), 2, pp. 546–554
[6] Hwnag, J.J., *et al.*, Experimental and Numerical Studies of Local Current Mapping on a PEM Fuel Cell, *International Journal of Hydrogen Energy*, *33* (2008), 20, pp. 5718–5727
[7] Pasaogullari, U., Wang, C.Y., Liquid Water Transport in Gas Diffusion Layer of Polymer Electrolyte Fuel Cells, *Journal of the Electrochemical Society*, *151* (2004), 3, pp. A399-A406
[8] Sedighizadeh, M., *et al.*, Parameter Optimization for a PEMFC Model with Particle Swarm Optimization, *International Journal of Engineering & Applied Sciences*, *3* (2011), 1, pp. 102-108
[9] Askarzadeh, A., Rezazadeh, A., Optimization of PEMFC Model Parameters with a Modified Particle Swarm Optimization, *International Journal of Energy Research*, *35* (2011), 14, pp. 1258-1265
[10] Mehrabi, M., *et al.*, Modeling of Proton Exchange Membrane Fuel Cell (PEMFC) Performance by Using Genetic Algorithm-Polynomial Neural Network (GA-PNN) Hybrid System, *Proceedings of the ASME*, 10th Fuel Cell Science, Engineering and Technology Conference, San Diego, 2012, pp. 1-6
[11] Tafaoli-Masoule, M., *et al.*, Optimum Design Parameters and Operating Condition for Maximum Power of a Direct Methanol Fuel Cell Using Analytical Model and Genetic Algorithm, *Energy*, *70* (2014), pp. 643-652
[12] Yang, W.J., *et al.*, Channel Geometry Optimization of a Polymer Electrolyte Membrane Fuel Cell Using Genetic Algorithm, *Applied Energy*, *146* (2015), pp. 1–10
[13] Sun, Z., *et al.*, Parameter Identification of PEMFC Model Based on Hybrid Adaptive Differential Evolution Algorithm, *Energy*, *90* (2015), pp. 1334-1341
[14] Al-Othman, A.K., *et al.*, Parameter Identification of PEM Fuel Cell Using Quantum-Based Optimization Method, *Arabian Journal for Science and Engineering*, *40* (2015), 9, pp. 2619-2628
[15] Haghighi, M., Sharifhassan, F., Exergy Analysis and Optimization of a High Temperature Proton Exchange Membrane Fuel Cell Using Genetic Algorithm, *Case Studies in Thermal Engineering*, *8* (2016), pp. 207–217
[16] Chen, X., *et al.*, Parametric Analysis and Optimization of PEMFC System For Maximum Power and Efficiency Using MOEA/D, *Applied Thermal Engineering*, *121* (2017), pp. 400-409
[17] Rao, S.S.L., *et al.*, Optimization of Operating Parameters to Maximize The Current Density Without Flooding At The Cathode Membrane Interface of a PEM Fuel Cell Using Taguchi Method And Genetic Algorithm, *International Journal of Energy and Environment*, 5 (2014), *3*, pp. 335-352
[18] Boudouh, M., *et al*, Experimental Investigation of Convective Boiling in Mini-Channels: Cooling Application of the Proton Exchange Membrane Fuel Cells, *Thermal Science*, *21* (2017), 1A, pp. 223-232
[19] Karimi, G., *et al.*, Along-Channel Flooding Prediction of Polymer Electrolyte Membrane Fuel Cells, *International Journal of Energy Research*, *35*(2011), 10, pp. 883-896
[20] Jamekhorshid, A., *et al.*, Current Distribution and Cathode Flooding Prediction in a PEM Fuel Cell, *Journal of the Taiwan Institute of Chemical Engineers*, *42* (2011), 4, pp. 622–631
[21] Nguyen, T.V., White, R.E., A Water and heat Management Model for Proton-Exchange-Membrane Fuel Cells, *Journal of the Electrochemical Society*, *140* (1993), 8, pp. 2178–2186
[22] Amani, M., Multi-Objective Optimization of Thermophysical Properties of Eco-Friendly Organic Nanofluids, *Journal of Cleaner Production*, *166* (2017), pp. 350-359
[23] Hemmat Esfe, M., Multi-Objective Optimization of nanofluid Flow in Double Tube Heat Exchangers for Applications In Energy Systems, *Energy*, *137* (2017), pp. 160-171
[24] Meidanshahi, V., Karimi G., Dynamic Modeling, Optimization and Control of Power Density in a PEM Fuel Cell, *Applied Energy*, *93* (2012), pp. 98-105
[25] Deb, K., *et al.*, A Fast and Elitist Multiobjective Genetic Algorithm: NSGA-II, *IEEE Transactions on Evolutionary Computation*, *6* (2002), 2, pp. 182-197